Available online at www.sciencedirect.com
SCIENCE DIRECT®
New Astronomy Reviews 50 (2006) 152–156
New Astronomy Reviews
www.elsevier.com/locate/newastrev

Luminosity functions and star formation rates at $z \sim 6$–10: Galaxy buildup in the reionization age

Rychard Bouwens *, Garth Illingworth

Department of Astronomy, University of California, Santa Cruz, 1156 High Street, Santa Cruz, CA, United States

Available online 4 January 2006

Abstract

HST ACS and NICMOS data are now of sufficient depth and areal coverage to place strong constraints on the formation and evolution of galaxies during the first 1–2 Gyrs of the universe. Of particular interest are galaxies at $z \sim 6$ since they represent the earliest epoch accessible to current high-efficiency optical instrumentation. To this end, we have been involved in the systematic construction of a large sample of 346 $z \sim 6$ objects from all the deepest wide-area HST data (UDF, UDF-Parallel, and GOODS fields). They have been used to construct an optimal determination of the rest-frame continuum UV LF at $z \sim 6$. Our LF extends to over 3 magnitudes below L^*, fainter than has been done at $z \sim 3$. Over the interval $z \sim 6$ to $z \sim 3$, we find strong evidence for evolution in the UV LF. Though we can thus far make no strong claims on an evolution of the faint end slope, the characteristic luminosity appears to have approximately doubled over the interval $z \sim 6$ to $z \sim 3$, consistent with hierarchical expectations. Remarkably, this shift to lower luminosities extends to even higher redshifts. Using all deep $J + H$ NICMOS observations (800 orbits in total), we have been able to demonstrate that the bright end of the LF ($> 0.3L^*_{z=3}$) is at least 5 times lower at $z \sim 10$ than at $z \sim 4$, with a similar deficit being established from our recent detections and first statistical sample of $z \sim 7$–8 galaxies using our UDF NICMOS data. In these precedings, we discuss what is known about the UV LF and UV luminosity density at $z \sim 6$–10 from current data and its evolution relative to $z \sim 3$. We also describe several exciting prospects for advance in this area over the next year.
© 2005 Elsevier B.V. All rights reserved.

PACS: 98.62.Ai; 98.62Qz; 98.62Ve; 98.80.Es

Keywords: Galaxies; High redshift; Luminosity functions; Star formation rates

Contents

1. Introduction . . . 153
2. $z \sim 6$ Rest-frame continuum UV LF . . . 153
3. First detections of $z \sim 7$–8 galaxies . . . 154
4. Searches for $z \sim 10$ galaxies . . . 154
5. Summary . . . 155
Acknowledgements . . . 156
References . . . 156

* Corresponding author.
E-mail addresses: bouwens@ucolick.org (R. Bouwens), gdi@ucolick.org (G. Illingworth).

1387-6473/$ - see front matter © 2005 Elsevier B.V. All rights reserved.
doi:10.1016/j.newar.2005.11.027

1. Introduction

Great progress has been made over the past few years in our observational understanding of galaxies at the end of the first billion years of the universe. Much of this progress has come at $z \sim 3$–6 and has been due in large part to the substantial gains in surveying efficiency made in the optical by the Advanced Camera for Surveys (ACS) on HST. This instrument provides us with a nearly ~10× increase in optical imaging efficiency over what was available with WFPC2, higher resolution imaging, and a reasonably efficient, red z-band filter. Putting together these capabilities with the well-established dropout technique (e.g., Steidel et al., 1996), it became possible to select literally hundreds to thousands of galaxies at redshifts of $z \sim 3$–6 (Bouwens et al., 2004b; Giavalisco et al., 2004) (see Fig. 1).

2. $z \sim 6$ Rest-frame continuum UV LF

Experience over the past two years has shown that a simple $i - z > 1.3$ color selection is remarkably effective at isolating galaxies at $z \sim 6$ (Stanway et al., 2003; Bouwens et al., 2003b; Dickinson et al., 2004). Though a small fraction of the selected sources are found to be low mass stars and low-redshift galaxies, most of these contaminants can be eliminated by making some requirement on their stellarity (i.e., how pointlike they are) or their flux in a bluer band (e.g., the V_{606}-band). These results have now been verified spectroscopically down to $z_{850,AB} \sim 27.5$ (Malhotra et al., 2005; Stanway et al., 2004; Dow-Hygelund et al., 2005).

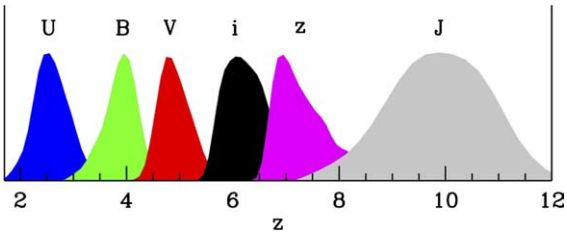

Fig. 1. Estimated redshift distributions for fairly standard U, B, V, i, z, and J-dropout selections. The standard suite of HST bands (e.g., F300W, F435W, F606W, F775W, F850LP, F110W) are used for these selections.

With this increasing understanding of the i-dropout selection, different studies attempted to construct rest-frame continuum UV (~1350 Å) luminosity functions (LFs) at $z \sim 6$ (Bouwens et al., 2004a; Bunker, 2004; Yan and Windhorst, 2004; Malhotra et al., 2005). Despite small differences in detail, each of these studies find that there were significantly fewer galaxies at $z \sim 6$ (per volume element) than at $z \sim 3$. A recent determination of this LF by our team is shown in Fig. 2(a) and incorporates the results from some ~350 i-dropouts selected from the two GOODS fields, two ACS parallel fields to the UDF, and the UDF (Bouwens et al., 2006). For comparison, we have also plotted the $z \sim 3$ LF (Steidel et al., 1999), and it is amazing to note that the $z \sim 6$ LF extends fainter than at $z \sim 3$, demonstrating the remarkable surveying efficiency of current optical instrumentation. It is also evident that our $z \sim 6$ LF shows a much larger deficit at the bright end than at the faint end, suggesting that high redshift galaxies are of much lower luminosity (on average). This explains (at least in part) why early searches down to brighter limiting magnitudes (Stanway et al., 2003) found more substantial evolution than similar searches down to fainter magnitudes (Bouwens et al., 2003b; Giavalisco et al., 2004).

We can look at this evolution in the rest-frame UV LF more quantitatively. In Fig. 2(b), we plot the likelihood contours for the $z \sim 6$ LF and contrast it with the equivalent values at $z \sim 3$ (thick black cross). The red and orange shaded regions on this plot indicate those Schechter parameters which are ruled out at 95% confidence using the current HST data and the HST data + Subaru data of Shimasaku et al. (2005), respectively. Though the constraints

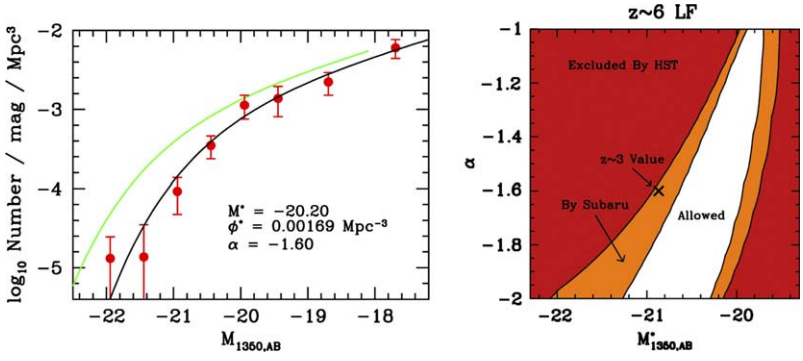

Fig. 2. The rest-frame continuum UV (~1350 Å) LF estimated from the UDF, the UDF-Ps, and the GOODS fields, shown in terms of the best-fit stepwise parameterizations (*red circles* with 1σ errors) and Schechter function (*solid black line*). The $z \sim 3$ LF is shown for comparison (*thick green line*) (Steidel et al., 1999). Our $z \sim 6$ LF shows a clear turnover at the bright end relative to the $z \sim 3$ LF and suggests that there has been a shift in the characteristic luminosity from $z \sim 6$ to $z \sim 3$. *(right panel)*. The allowed regions of parameter space (95% confidence) for the $z \sim 6$ LF using current HST data (Bouwens et al., 2006) and current HST data combined with a bright Subaru search (Shimasaku et al., 2005). The equivalent $z \sim 3$ values are shown with the large cross. Though no constraint can be placed on the faint-end slope α at $z \sim 6$, the characteristic luminosity at $z \sim 6$ appears to be ~0.7 mags fainter than at $z \sim 3$. (For interpretation of the references to the color in this figure legend, the reader is referred to the web version of this article.)

on the faint-end slope α at $z \sim 6$ are still somewhat modest, the preferred values for the characteristic luminosity M^*_{UV} are much lower than at $z \sim 3$, suggesting that there has been evolution in the characteristic scales on which star formation is occurring. This provides us with one of our first, most direct evidences for the hierarchical buildup of galaxies early in the history of the universe. (see also Davé, this meeting and Yan and Windhorst, 2004). Further refinements to the $z \sim 6$ LF should be forthcoming over the next year. In part, this will be due to an inclusion of a much deeper set of GOODS images in the analysis and in part due to two additional deep fields that will be taken with ACS during HST Cycle 14 (GO-10632).

3. First detections of $z \sim 7$–8 galaxies

Extending the dropout search beyond $z \sim 6$ requires the detection of objects in the infrared. This has been difficult due to the well-known limitations of infrared technology and because $z \sim 7$–8 objects are likely to be very faint. At $z \sim 6$, the characteristic luminosity we estimate is nearly 0.7 mag fainter than at $z \sim 3$. Extrapolated to even higher redshift, the characteristic luminosities we expect are likely to be even fainter still, perhaps 0.3 $L^*_{z=3}$. In the H-band, this corresponds to a magnitude of 27.3, which can only be reached in deep NICMOS studies and very deep ground-based studies around massive lensing clusters.

The deep NICMOS imaging over the optical UDF provided us with one of our first opportunities to find $z \sim 7$–8 galaxies. The 5σ limiting depths in these data were 27.6 in the J_{110}-band and 27.4 in the H_{160}-band. Moreover, the optical data for this field were more than sufficient to set strong constraints on the z_{850} band fluxes. Using a relatively aggressive object detection, we carried out a z_{850}-dropout selection on these data and found 5 $z \sim 7$–8 candidates. Successive tests on our selection – including scattering experiments and selection on the negative images – suggested that most of our 5 candidates were likely at $z \sim 7$–8 and we had only one likely contaminant. We therefore adopted as our likely sample 4 fiducial candidates (see Fig. 3).

To assess the implications of this first statistical sample of $z \sim 7$–8 objects, we generated no-evolution predictions based upon a lower redshift $z \sim 3.8$ B_{435}-dropout sample (Bouwens et al., submitted for publication-a) using our well-established cloning machinery (Bouwens et al., 1998, 2003a, submitted for publication-b). An important thing to account for in projecting these lower redshift samples to high redshifts was the observed evolution in size (Ferguson et al., 2004; Bouwens et al., 2004b) and UV color (Stanway et al., 2005; Bouwens et al., 2006). Running through these simulations, a total of 14 objects are expected. We compared this prediction with 4 fiducial objects, given the expected small but non-zero contamination. This suggested that the rest-frame UV ($\sim$1600 Å) luminosity density at $z \sim 7$–8 was just 0.28× that at $z \sim 3.8$ (number weighted) or 0.20× the $z \sim 3.8$ value (if we use a luminosity weighting).

Though a first estimate of the rest-frame UV luminosity density at $z \sim 7$–8, we would like to emphasize that our determination still suffers from some substantial uncertainties, notably the Poissonian errors ($\pm$50%), cosmic variance (factor of 2), as well as the overall contamination level ($\sim$0–2 objects). This situation should improve substantially over the next year using data from two HST programs: (1) a deep z_{850}-dropout search in the field (GO-10632) and (2) a similar search around seven massive lensing clusters (GO-10504 and GO-10699). Both should yield $\sim$10 $z \sim 7$–8 candidates, substantially reducing uncertainties from our previously quoted estimates based on the HUDF NICMOS footprint. Simultaneously, searches with large ground-based telescopes are ongoing and have yielded a sizeable number of candidates, particularly around lensing clusters (Mannucci et al., in preparation; Richard et al., submitted for publication).

4. Searches for $z \sim 10$ galaxies

The detection and confirmation of galaxies at $z \sim 10$ appears to be a significantly more difficult endeavor than even galaxies at $z \sim 7$–8. Though the additional distance

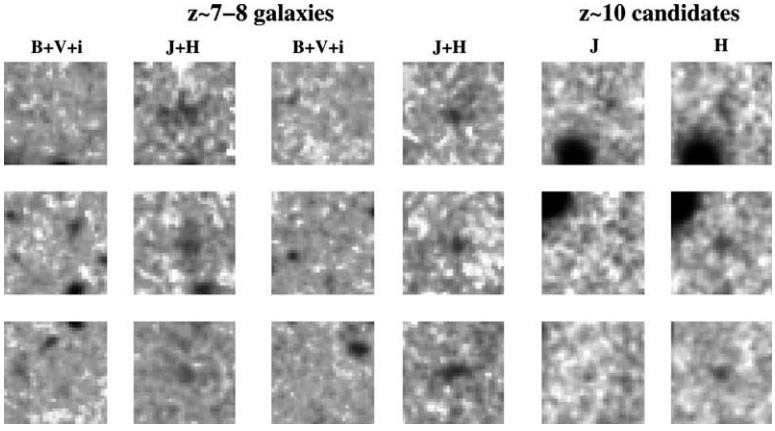

Fig. 3. Candidate $z \sim 7$–8 and $z \sim 10$ galaxies from the UDF NICMOS footprint and NICMOS parallels to the UDF (Bouwens et al., 2004c, 2005).

plays a small role, by far the biggest challenge is their luminosity: $z \sim 10$ galaxies are expected to have very low luminosities, several times lower than at $z \sim 6$ or $z \sim 7$–8 (Cooray, submitted for publication; Davé, this meeting). Even assuming no evolution in luminosity from $z \sim 7$–8 to $z \sim 10$, typical magnitudes for these objects would be ~28 in the H-band, suggesting that one would need to probe to very faint magnitudes indeed.

One way of probing to such magnitudes is to use the very deep IR imaging capabilities of the HST NICMOS camera. Unfortunately, even with this instrument, searches for $z \sim 10$ objects are still extremely expensive, e.g., ~150 orbits are needed to detect just one $z \sim 10$ object, and this assumes that the UV LF does not evolve from $z \sim 10$ to $z \sim 6$. It is thus no surprise that there has been a lack of dedicated searches. Nevertheless, it is possible to take advantage of the deep J_{110} and H_{160} parallel data associated with several HST deep fields to conduct a search. Such data are available for the HDF-S (150 orbits) and the UDF (~340 orbits). There is also deep NICMOS $J + H$ imaging over the WFPC2 HDF-N (176 orbits) and a portion of the ACS UDF (144 orbits). The 5σ limiting magnitudes of these data range from $H_{160,AB} \sim 27$ to $H_{160,AB} \sim 28.5$, which is sufficient to identify $z \sim 10$ galaxies down to $0.3L^*_{z=3}$ (see Fig. 4).

To see what we could learn from these data, we carried out a search for $(J_{110} - H_{160})_{AB} > 1.8$ J-dropouts and found 11 objects (Bouwens et al., 2005). We eliminated those objects with 2σ detections in the optical bands or with $H - K$ colors substantially redder than the typical starburst type object (i.e., UV continuum slopes $\beta > 0.5$). This left us with 3 candidates, all of whom are in the NICMOS parallel fields to the UDF. Since we did not have comparably deep images blueward or redward of the $J_{110}H_{160}$ passbands, it was difficult to be very sure about the redshifts of our 3 candidates. Nevertheless, we could still compare these three candidates with the numbers expected assuming no-evolution from $z \sim 6$. Repeating the simulations described in Section 3 we obtained 4.8 J_{110}-dropouts, only somewhat higher than our 3 candidates. We consider two extreme cases. If we assume that all three candidates are at $z \sim 10$, the volume densities we obtain at $z \sim 10$ is just $0.7 \pm 0.3\times$ that at $z \sim 6$. If, however, we assume that none of these candidates are at these redshifts, the volume densities we obtain are just $<0.2\times$ the $z \sim 6$ value (1σ). Remarkably, we found that these results were not very sensitive to cosmic variance (~19% RMS) due to the extremely large comoving distances probed in these pencil beam searches (~500 Mpc).

The current round of HST proposals should strengthen these constraints significantly. Not only will we add about 60% to the total NICMOS observing time relevant to these searches (further improving our statistics), but some very deep ACS observations (~28.5 mag at 5σ for apertures that match the NICMOS data) will be taken over the deep NICMOS parallels containing our 3 $z \sim 10$ candidates. Independent searches are also ongoing around lensing clusters (GO-10380, GO-10504, GTO-10699, and (Mannucci et al., in preparation)), and we note that there are claims by some teams to have a set of very good candidates.

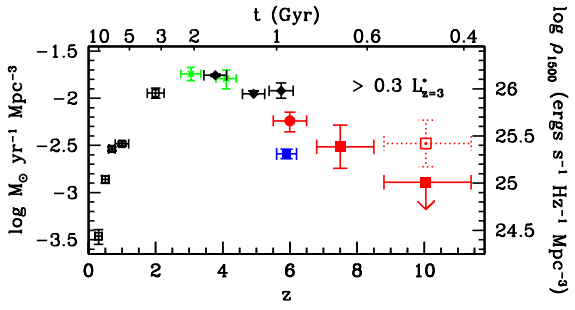

Fig. 4. The cosmic star formation rate density versus redshift with no extinction correction. The star formation rate density (integrated down to $0.3\,L^*_{z=3}$ – the limit of our $z \sim 7$–8 and $z \sim 10$ searches) was calculated from the luminosity density in the rest-frame UV continuum (~1500 Å: plotted on the right vertical axis) using canonical assumptions and a Salpeter IMF (Madau et al., 1998). The open red square at $z \sim 10$ shows our result if 3 objects from this study prove to be at $z \sim 10$, while the large downward pointing arrow shows our 1σ limits if none are (Bouwens et al., 2005). Included on this plot are also estimates by Schiminovich et al. (2005) (open black squares), (Steidel et al., 1999) (green crosses), (Giavalisco et al., 2004) (black diamonds), (Bunker, 2004) (solid blue square), (Bouwens et al., 2004c) (solid red square), and (Bouwens et al., 2006) (solid red circle). (For interpretation of the references to the color in this figure legend, the reader is referred to the web version of this article.)

5. Summary

Current observations are now of sufficient quality to robustly determine the rest-frame UV (~1350 Å) luminosity function at $z \sim 6$. These determinations extend to nearly three magnitudes below L^*, fainter than has been possible at $z \sim 3$, demonstrating the efficiency of current optical technology. Substantial changes are evident in the LF relative to $z \sim 3$, suggesting that typical galaxies have more than doubled their star formation rates over this interval. The observed evolution is suggestive of that expected from popular hierarchical models, and would seem to indicate that we are literally seeing the buildup of galaxies over this range.

Progress with higher redshift dropout samples has been less dramatic, but is still forthcoming. Our sample of $z \sim 7$–8 z_{850}-dropouts in the HUDF provided our first statistical sample of galaxies in this epoch and thus allowed an initial estimate of the luminosity density in this era (Bouwens et al., 2004c). Searches for higher redshift $z \sim 10$ J-dropouts have resulted in some candidates as well as yielding some useful upper limits on the bright end of the UV LF. Galaxies at both times stand to undergo notable improvements as the result of future and ongoing programs. Of course, for truly substantial gains in this area, we will need to wait for the availability of high resolution, high sensitivity space-based imagers, such as WFC3 or NIRCam (JWST).

Acknowledgements

We are indebted to the many members of the ACS GTO and UDF NICMOS GO teams for their contribution to the current research. Of particular note was the assistance provided by John Blakeslee, Daniel Eisenstein, Marijn Franx, Rodger Thompson, and Pieter van Dokkum, each of whom contributed in an extremely important way. We also acknowledge valuable discussions with Brandon Allgood, Tom Broadhurst, Andy Bunker, Akio Inoue, Sangeeta Malhotra, James Rhoads, Evan Scannapieco, Daniel Schaerer, and Jason Tumlinson. ACS was developed under NASA Contract NAS5-32865, and this research was supported under NASA Grants HST-GO09803.05-A and NAG5-7697.

References

Bouwens, R.J. et al., 1998. Astroph. J. 506, 557.
Bouwens, R.J. et al., 2003a. Astroph. J. 593, 640.
Bouwens, R.J. et al., 2003b. Astroph. J. 595, 589.
Bouwens, R.J. et al., 2004a. Astroph. J. Letters 606, L25.
Bouwens, R.J. et al., 2004b. Astroph. J. Letters 611, 1.
Bouwens, R.J. et al., 2004c. Astroph. J. Letters 616, L79.
Bouwens, R.J. et al., 2005. Astroph. J. Letters 624, L5.
Bouwens, R.J., et al., submitted for publication-a. Astroph. J.
Bouwens, R.J., et al., submitted for publication-b. Astroph. J.
Bouwens, R.J., et al., 2006. astro-ph/0509641, in press.
Bunker, A.J., 2004. MNRAS 355, 374.
Cooray, A., MNRAS 364, 303.
Davé, R., this meeting.
Dickinson, M. et al., 2004. Astroph. J. Letters 600, L99.
Dow-Hygelund, C. et al., 2005. Astroph. J. Letters 630, 137.
Ferguson, H.C. et al., 2004. Astroph. J. Letters 600, L107.
Giavalisco, M. et al., 2004. Astroph. J. Letters 600, L103.
Madau, P. et al., 1998. MNRAS 498, 106.
Malhotra, S. et al., 2005. Astroph. J. 626, 666.
Mannucci, F., et al., in preparation.
Richard, J., et al., submitted for publication. Astron. & Astroph.
Schiminovich, D. et al., 2005. Astroph. J. Letters 619, 47.
Shimasaku, K. et al., 2005. PASJ 57, 447.
Stanway, E.R. et al., 2003. MNRAS 342, 439.
Stanway, E.R. et al., 2004. AstroPh. J. Letters 604, L13.
Stanway, E.R. et al., 2005. MNRAS 359, 1184.
Steidel, C.C. et al., 1996. Astroph. J. Letters 462, L17.
Steidel, C.C., Adelberger, K.L., Giavalisco, M., Dickinson, M., Pettini, M., 1999. Astroph. J. 519, 1.
Yan, H., Windhorst, R.A., 2004. Astroph. J. Letters 612, L93.